

# Population-Scale Network Embeddings Expose Educational Divides in Network Structure Related to Right-Wing Populist Voting

Malte Lüken<sup>1,2,3\*</sup>, Javier Garcia-Bernardo<sup>4,5</sup>, Sreeparna Deb<sup>6</sup>, Flavio Hafner<sup>1,3</sup>,  
and Megha Khosla<sup>7</sup>

<sup>1</sup>Netherlands eScience Center, The Netherlands

<sup>2</sup>Department of Psychology, University of Amsterdam, The Netherlands

<sup>3</sup>Erasmus School of Behavioral and Social Sciences, Erasmus University Rotterdam, The Netherlands

<sup>4</sup>ODISSEI Social Data Science Team, Department of Methodology and Statistics, Utrecht University, The Netherlands

<sup>5</sup>Centre for Complex System Studies, Utrecht University, The Netherlands

<sup>6</sup>Department of Software Technology, Delft University of Technology, The Netherlands

<sup>7</sup>Department of Intelligent Systems, Delft University of Technology, The Netherlands

## ABSTRACT

Administrative registry data can be used to construct population-scale networks whose ties reflect shared social contexts between persons. With machine learning, such networks can be encoded into numerical representations—embeddings—that automatically capture individuals’ position within the network. We created embeddings for all persons in the Dutch population from a population-scale network that represents five shared contexts: neighborhood, work, family, household, and school. To assess the informativeness of these embeddings, we used them to predict right-wing populist voting. Embeddings alone predicted right-wing populist voting above chance-level but performed worse than individual characteristics. Combining the best subset of embeddings with individual characteristics only slightly improved predictions. However, after transforming the embeddings to make their dimensions more sparse and orthogonal, we found that one embedding dimension was strongly associated with the outcome. Mapping this dimension back to the population network revealed differences in network structure related to right-wing populist voting between different school ties and achieved education levels. Our study contributes methodologically by demonstrating how population-scale network embeddings can be made interpretable, and substantively by linking structural network differences in education to right-wing populist voting.

---

\*Corresponding author. Email: m.luken@esciencecenter.nl.

## Introduction

Combining administrative registry data with machine learning has opened new opportunities for social science research [1, 2, 3, 4, 5, 6, 7]. A recent example is *life2vec*, a deep learning model trained on life sequences from Danish registry data spanning the entire Danish population that improved predictions of life events such as early mortality substantially [8]. Another recent example is the *PreFer* data challenge, in which researchers used a combination of registry and survey data from the Dutch population to predict childbirth at the individual level [9].

To make accurate predictions, deep learning models typically encode input data into latent numerical representations—so-called embeddings [10, 11]. Their goal is to reduce the dimensionality while also preserving the structure and non-linear relationships of complex input data. In contrast to hand-crafted features, embeddings capture the structure of complex inputs automatically from the data. Within the social sciences, this is especially relevant in networks [12] since the position of persons within social networks impacts social outcomes (e.g., economic [13], health-related [14], and political [15]), and capturing such position using hand-crafted features is particularly difficult [16].

Registry data contain information about shared social contexts between persons that can be used to construct networks at population-scale [17, 18, 19]. For example, when people live in the same household or work for the same employer, this shared social context can be indicated by a network tie. While such ties do not measure direct interaction, they reflect an increased probability of contact and shared exposure to contextual factors [20]. In this study, we draw on a recently released network based on Dutch registry data comprising *all* persons living in the Netherlands [17]. This network records relational ties representing five social contexts, namely neighbors, colleagues, family, classmates, and household, for 17.4 million residents, totaling 1.4 billion connections.

Using the population network, we created embeddings for the entire Dutch population solely based on shared social contexts (Fig. 1A). The embeddings encode each person’s position within the network, capturing complex connectivity patterns and structural roles in a compact representation. The goal of this study was to gain insight into the information the embeddings contain about a relevant social outcome—right-wing populist voting (Fig. 1B)—and the structural patterns in the network associated with it (Fig. 1C). In the preregistered part of our study, we therefore used the embeddings to predict right-wing populist voting and tested whether they improved predictions based on individual characteristics.

We chose right-wing populist voting behavior as the social outcome to evaluate the informativeness of our embeddings for two reasons: First, the last Dutch parliamentary election on November 22nd, 2023, yielded an unprecedented high turnout for right-wing populist parties [21]. For the first time in Dutch history, a right-wing populist party (*Partij voor de Vrijheid*; PVV) was part of the government coalition. Second, decades of research have documented a link between social relations and voting behavior [22, 23, 24, 25, 26, 27, 28, 29, 30], including experimental evidence that voting behavior is contagious [31]. Taken together, we expected to observe a stronger influence of network position on this particular outcome. Because the Dutch registry does not contain data on voting behavior at the individual level, we linked it with survey data from a representative sample ( $N = 6,063$ ) of the Dutch population [32] that contains such information.

A key limitation of standard embeddings is that they are not inherently interpretable: the dimensions of the embeddings are often highly correlated, and there is no guarantee that dimensions

of the embedding space correspond to meaningful, observable external variables or social outcomes [33]. In the exploratory part of our study, we addressed this challenge by applying the Dimensional Interpretability of Node Embeddings (DINE) framework [34] to disentangle embedding dimensions. The DINE framework uses regularizing auto-encoders to enforce sparsity and orthogonality in the embedding dimensions, making them more distinct and easier to interpret. Mapping the dimensions that are most predictive of the outcome back to the population network allowed us to investigate which structural patterns are associated with right-wing populist voting.

The embeddings alone predicted right-wing populist voting better than chance-level, but they performed worse than models based on individual characteristics and improved predictions only slightly when combined with them. However, embeddings offer a lens into which structural patterns in the network are linked to right-wing populist voting, which is not possible using individual characteristics alone. Our interpretability analysis revealed that one embedding dimension was particularly important for predicting right-wing populist voting. We mapped this “populist” dimension to the population network and found strong differences in local network structure between school relations and levels of achieved education that were predictive of right-wing populist voting.

Our study makes a methodological contribution by demonstrating how populations-scale network embeddings can be made interpretable. It also makes a substantial contribution by showing how populations-scale network embeddings, while only slightly improving predictions, give insight into structural network differences in education that are predictive of right-wing populist voting. This highlights the potential of interpretability methods for researchers to gain a deeper understanding of the link between network structure and social outcomes.

## Results

### Pre-registered Analysis: Population Network Embeddings Predict Right-Wing Populist Voting

We start by addressing the question to what extent embeddings predicted right-wing populist voting and whether they improved predictions based on individual characteristics (covariates). Among prediction models with three different feature sets—embeddings-only, covariates-only, and embeddings-plus-covariates—, we expected embeddings-plus-covariates to perform better than embeddings-only and covariates-only, and feature sets including embeddings to outperform those not including embeddings. We used Bayesian regression and marginal effects to compare the out-of-sample performance (measured via macro AUC) of prediction models across several manipulations: feature sets, prediction algorithms (k-nearest neighbors, logistic regression, and XGBoost), network years (2020, 2021, and 2022), embedding methods (DeepWalk and LINE), embedding hyperparameters, and untransformed vs. DINE-transformed embeddings. Thus, all reported results are based on macro AUC scores *estimated* by the Bayesian regression. This approach allowed us to compute differences in prediction performance between feature sets aggregated over other manipulations.

Embeddings-only models showed the worst prediction performance, followed by embeddings-plus-covariates models (Fig. 2). While covariates-only models had the highest prediction performance. The difference between embeddings-only and covariates-only was  $\Delta\text{AUC} = 0.09$ , 95% CI [0.089, 0.090] while the difference between embeddings-only and embeddings-plus-covariates models was  $\Delta\text{AUC} = 0.077$ , 95% CI [0.077, 0.078]. Between covariates-only and embeddings-plus-covariates models, the difference was  $\Delta\text{AUC} = -0.012$ , 95% CI [-0.013, -0.012]. As we

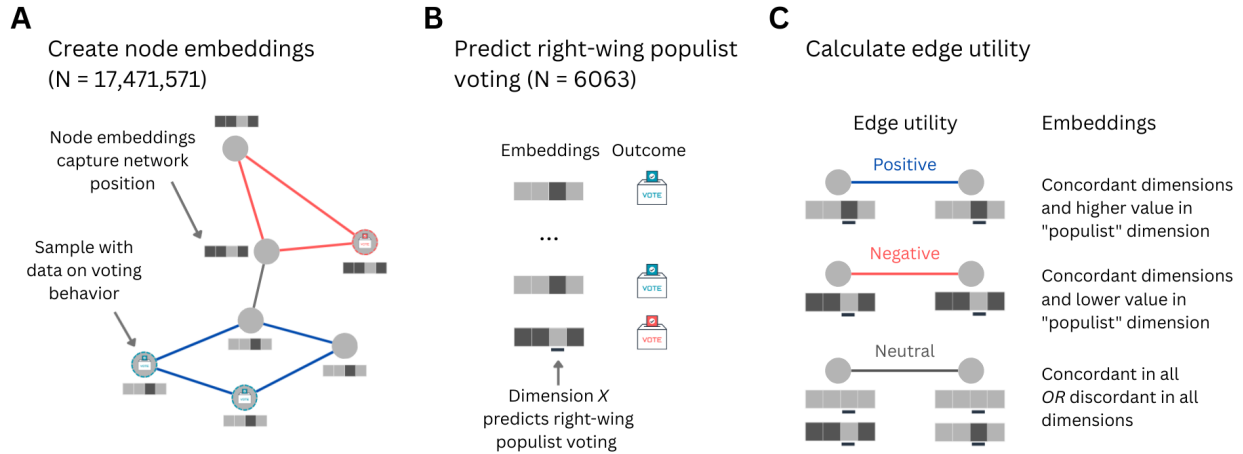


**Figure 1: Illustration of our approach.** A: We created node embeddings for all persons in the population network (here displayed with four dimensions). Persons that could be linked to their voting behavior are indicated with a dashed contour. B: For those individuals, we predicted right-wing populist voting using network embeddings and individual characteristics. We identified one dimension (underlined) that was highly predictive of right-wing populist voting. C: We computed edge utilities for the entire population network, indicating the importance of an edge for predicting right-wing populist voting. When two connected nodes are concordant in the embedding dimensions and have a high value in the selected dimension, edge utility is positive. When they are concordant in the embedding dimensions and have a low value in the selected dimension, edge utility is negative. When they are concordant *or* discordant in all dimensions, edge utility is zero.

will explore next, this is due to the inability of logistic regression and k-nearest neighbor models to effectively use the embeddings.

In Table A1, we show that, among the prediction algorithms, XGBoost outperformed logistic regression and k-nearest neighbors. Among the embedding methods and embedding hyperparameters, DeepWalk with 100 walks per node of length 20 and 32 embedding dimensions performed best; however, the differences in prediction performance were small. We did not observe differences in prediction performance between DINE-transformed and untransformed embeddings, embedding window sizes, or network years.

### Exploratory Analysis: Structural Network Differences in Education Related to Right-Wing Populist Voting

Because some embedding hyperparameters and prediction algorithms performed better than others, we compared prediction performance across feature sets within a subset of predictive models, namely, XGBoost using DeepWalk embeddings with 100 walks of length 20 with dimension 32. Aggregated over manipulations that did not show any difference in performance (untransformed vs. DINE-transformed embeddings, window sizes, and network years), the predicted performance was higher and embeddings-plus-covariates models were slightly better than covariates-only models,  $\Delta\text{AUC} = 0.011$ , 95% CI [0.0094, 0.012] (Fig. 2).

For the remainder of our exploratory analysis, we selected the DINE-transformed embeddings from the prediction model with the highest prediction performance score (see Table A2).

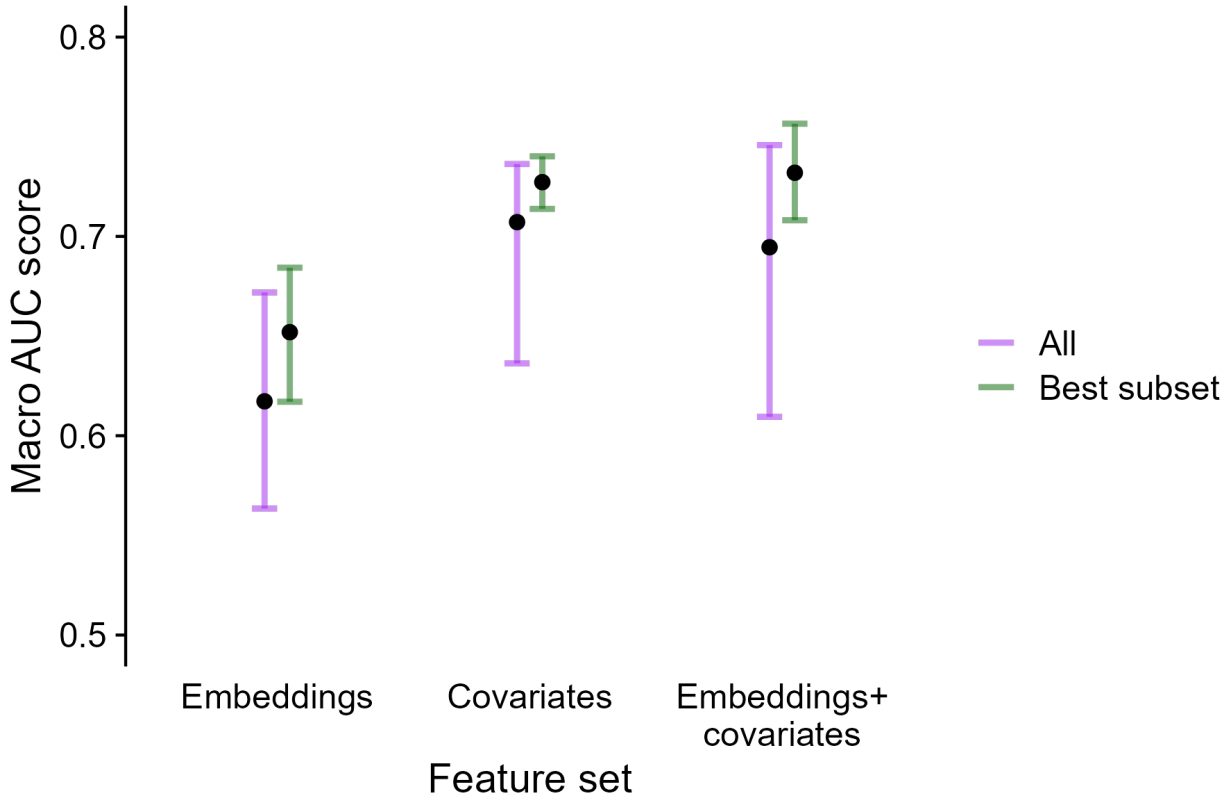


Figure 2: **Out-of-sample prediction performance for right-wing populist voting.** Performance was measured with the macro AUC score (on y-axis). The x-axis shows different feature sets used for prediction. Points indicate the out-of-sample posterior predictive mean. Vertical bars indicate 95% credible intervals. Colors indicate whether the predictions were made for all scores (purple) or only for a subset of the best performing prediction models (XGBoost and embeddings with 100 walks per node of length 20 and 32 embedding dimensions, green).

### One Embedding Dimension Is Strongly Associated With Populist Voting

After observing that network embeddings predicted right-wing populist voting, we investigated whether embedding dimensions differed in their importance for prediction. The regularizing auto-encoder in the DINE framework transforms embedding dimensions to become orthogonal and sparse (see Methods for details). We therefore expected the feature importance of DINE-transformed embeddings to be concentrated in fewer dimensions.

To understand the effect of the DINE-transformation and of combining embeddings with covariates, we examine SHAP values that measure the contribution of each feature to the model’s predictions for the three feature sets (covariates-only, embeddings-only, embeddings-plus-covariates) when the embeddings were untransformed and when they were transformed using DINE (Fig. 3).

Starting with a prediction model using only covariates (Fig. 3A), we observed that the highest achieved education levels and trust in the government were the most important predictors, followed by optimism, interpersonal trust, and gender. Highest achieved vocational education, lower trust in the government, lower optimism, and lower interpersonal trust increased the predicted probability of voting for a right-wing populist party.

We also compared embeddings-only prediction models (Fig. 3B). As expected, we observed that the model with untransformed embeddings had SHAP values evenly distributed across dimensions. This suggests that they were roughly equally important for predicting populist voting. For models with DINE-transformed embeddings, SHAP values were larger for dimension 17 than for other dimensions, indicating that this dimension was more important than others.

Next, we compared models that included both embeddings and covariates (Fig. 3C). In the model with untransformed embeddings, multiple embedding dimensions had relatively small SHAP values. In the model with DINE-transformed embeddings, dimension 17 had much larger values than the other dimensions, being the second most important predictor after trust in the government.

### Structural Differences in “Populist” Embedding Dimension

**Individual Level** Because dimension 17 was the main DINE-embedding dimension predictive of right-wing populist voting, we selected it to calculate utility scores for all edges in the population network. Edge utility indicates the *marginal* contribution of dimension 17 to the average similarity overall all dimensions between the source and target node embeddings (see Methods for details). Positive values mean that either all dimensions are concordant but dimension 17 has a higher value than the others or dimension 17 is concordant and the other dimensions are discordant. In contrast, negative values indicate that either all dimensions are concordant but dimension 17 has a lower value than the other dimensions or dimension 17 is discordant and the other dimensions are concordant. In our case, edge utility reflects the importance of an edge for predicting right-wing populist voting.

We compared edge utility between different relation types in the population network. Most relation types had an average edge utility close to zero (Fig. 4) suggesting in general little importance of dimension 17. However, four relations had shifted (positive or negative) edge utility. Institutional household relations had more negative average edge utility compared to non-institutional households and other relation types (Fig. 4A). For classmate relations, we observed more positive average edge utility for university relations and more negative average edge utility for vocational and special school relations (Fig. 4B). This indicates that institutional household, vocational school, special school, and university relations were important for predicting right-wing populist voting. Given that persons with a lower achieved education level and lower values in dimension 17 were more likely and persons with a higher achieved education level and higher values in dimension 17 were less likely to vote for a right-wing populist party in the LISS panel data (Fig. 3), we reason that university relations connected persons with concordant embedding dimensions but high values in dimension 17. Conversely, vocational and special school relations connected persons with concordant embedding dimensions but low values in dimension 17. This implies that persons connected through university and vocational/special schools were more likely to have concordant voting behavior for non-populist and right-wing populist parties, respectively. It also means that there is a similarity in local network structure between persons connected through these relations that is captured by dimension 17.

Alternatively, this result could mean that persons connected through university relations were discordant in all embedding dimensions except for dimension 17. This would imply that they were dissimilar in local network structure except for the part predictive of right-wing populist voting. Similarly, persons connected through vocational/special school and institutional household relations could have been discordant in dimension 17 but concordant in the other embedding di-

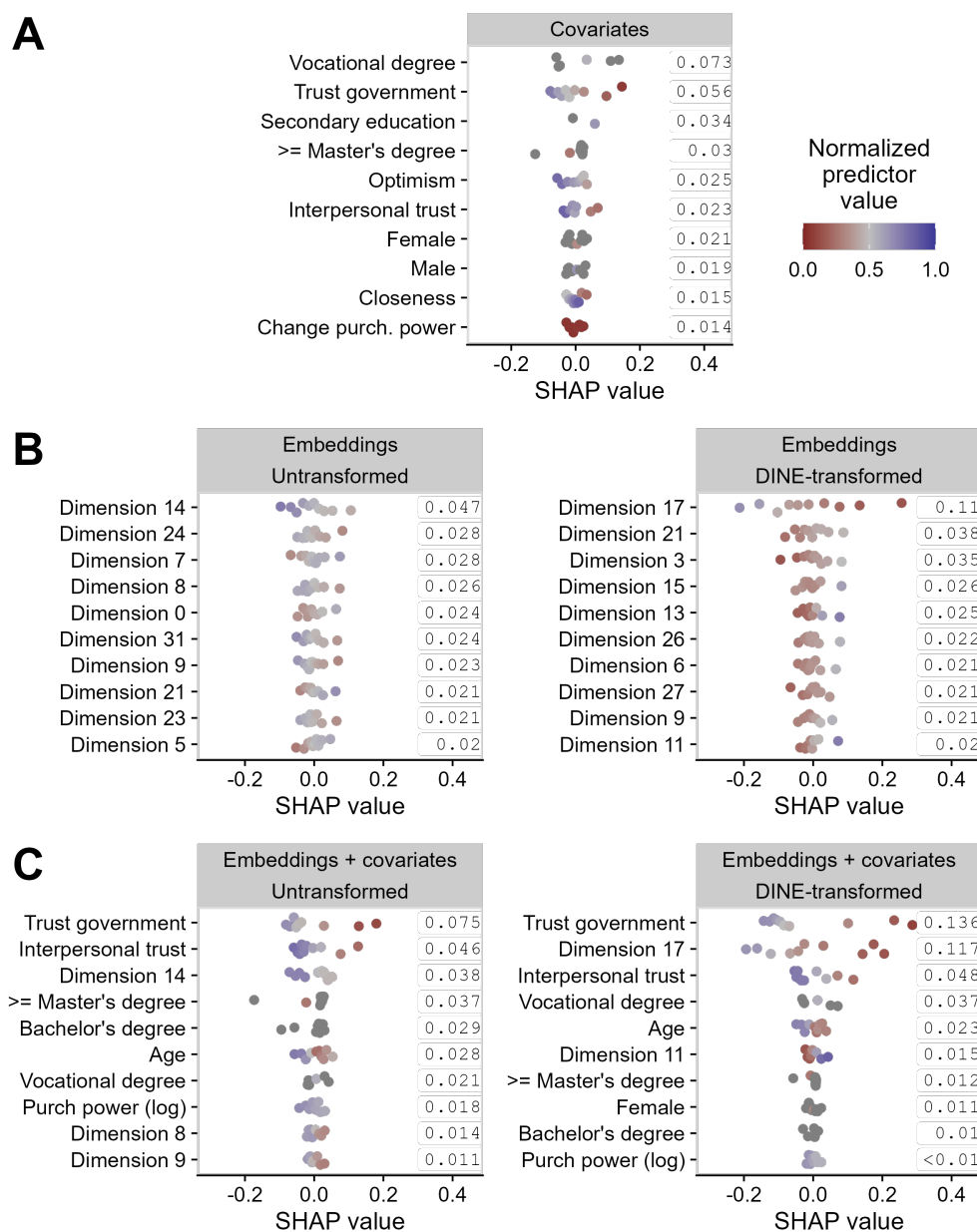


**Figure 3: Importance of 10 most important variables predicting populist voting behavior in the LISS panel data.** Importance was quantified with SHAP values for each predictor and observation. Individual SHAP values were aggregated for each decile to guarantee privacy of the panel subjects. Each point represents the average SHAP value of a decile. Color indicates the average SHAP value in the decile, normalized between zero and one. Grey-colored points indicate that the average value could not be published to prevent group disclosure. Predictors on the y-axis are ordered according to the mean of their absolute decile-averaged SHAP values which are displayed on the right side of each panel. Panels contain results for predictor sets that included (A) only covariates (B) only embeddings or (C) embeddings and covariates. For (B–C), the results with untransformed versus DINE-transformed embeddings is shown in the two columns.

mensions. That is, they could have had similar local network structure except for the part predictive of right-wing populist voting. We argue that this interpretation is plausible for a small subset of the relations but less so for the entire population (see also Municipality Level and Discussion).

Next, we looked at the importance of relations in each person's ego-network measured by edge utility strength, i.e., the sum of the edge utility each person's first-order relations (Fig. 5). Edge utility strength measures the structural similarity between a person and its first-order neighbors that is associated with right-wing populist voting. We observed differences in edge utility strength between achieved education levels but no differences for the number of parents born abroad or gender. For achieved education, the results show that persons who obtained a Master's/doctorate or Bachelor's degree had on average positive and those with a vocational degree had negative utility strength. Persons who had achieved a primary, secondary, or unknown education level had average edge utility close to zero. This pattern indicates that first-order relations were more important for predicting right-wing populist voting for persons with university and vocational achieved education levels. It suggests that persons with university and vocational education had concordant embedding dimensions with their neighbors but high and low values in dimension 17, respectively. In other words, there were differences in local network structure between university and vocational education levels that were predictive of right-wing populist voting and captured by dimension 17.

However, there is an alternative interpretation that persons with university education were dissimilar and persons with vocational education similar in local network structure to their neighbors except for the part predictive of right-wing populist voting. Again, we argue that this interpretation might hold for a small part but not for the entire population.

We also looked at Pearson correlations between edge utility strength and age as well as gross income percentile which were both small (age:  $r = -0.05$ ; income:  $r = 0.08$ ), suggesting little difference in structural similarity.

**Municipality Level** Because prior research has shown differences in the dynamics of populist voting behavior at the micro- and macro-level [35], we extended our analysis to the municipality-level. Moreover, aggregated voting results were publicly available at the municipality level, allowing us to link aggregated edge utility and right-wing populist voting directly. That is, we computed the average edge utility between persons residing in the same or in a different municipality in the Netherlands. For each municipality, we then calculated the strength of the average edge utility. The strength reflects the average importance of persons' relations for predicting right-wing populist voting in a municipality. We correlated the average edge utility strength with municipality level statistics, including right-wing populist votes. Figure 6A shows that municipalities with more highly educated inhabitants, higher income, higher address density (i.e., more urban), and more inhabitants with non-western migration background had higher average edge utility strength, suggesting higher importance for right-wing populist voting. Thus, residents in higher education, income, and address density municipalities had concordant embedding dimension with their network neighbors and high values in dimension 17, whereas residents in lower and intermediate education municipalities had concordant embedding dimension with their network neighbors and low values in dimension 17. Age groups, household assets, and migration background had low correlations with average edge utility strength and, thus, were less important at the municipality level.

Figure 6B shows correlations between municipality statistics and right-wing populist votes. Education levels had the strongest correlations ( $|r| \approx 0.8$ ), followed by average edge utility strength



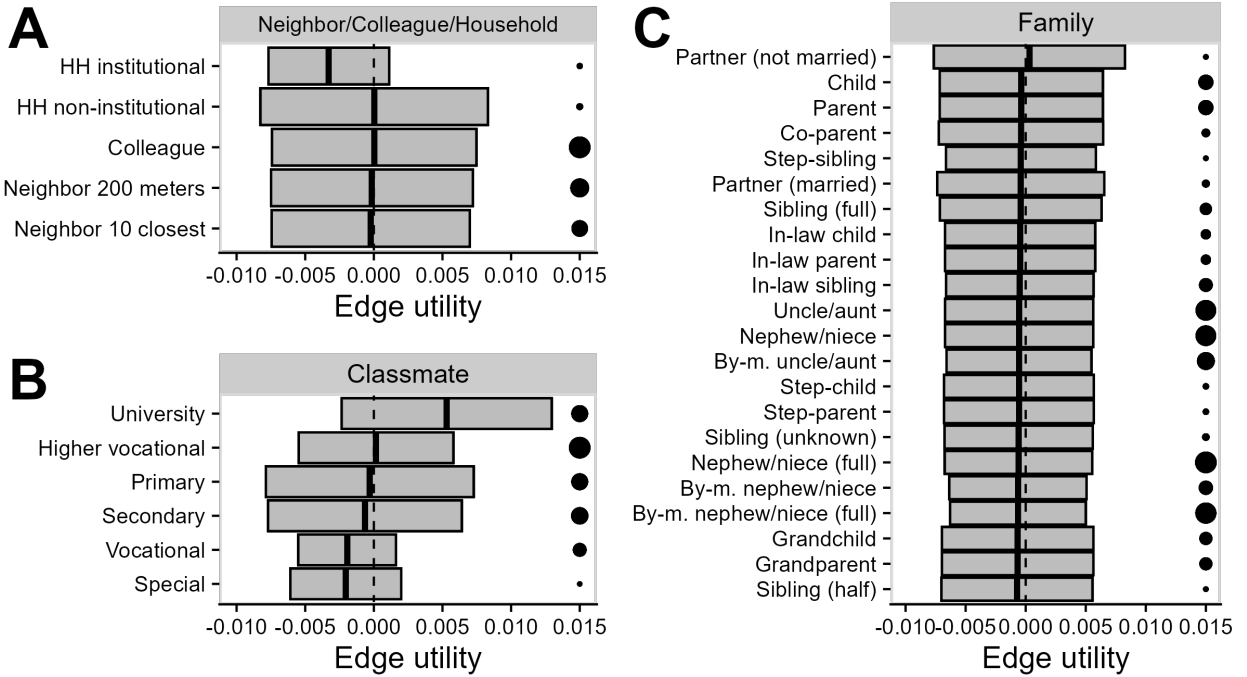


**Figure 4: Edge utility scores (x-axis) for different network relation types (y-axis) and relation groups.** Bold vertical bars indicate means and boxes span  $\pm 2$  standard deviations from the mean of the edge utility distributions of (A) neighbors, colleagues and households, (B) classmates, and (C) family relations. The size of the circles on the right of each box indicate the number of relations of the respective type. Classmate relations typically refer to students enrolled at the same school in the same location in the same school year (but this differs per relation type). Special schools are dedicated to students with mental, physical, or learning disabilities. Examples for institutional households are elderly homes, student dorms, and prisons. For neighbor relations, 200 meters refers to 20 random persons living within a 200 meter radius and 10 closest refers to 10 random persons living at the closest addresses. HH = household. By-m. = related by marriage.

and income( $|r| \approx 0.6$ ). Thus, average edge utility strength was strongly associated with right-wing populist voting at the municipality level. This association supports our interpretation in the individual-level analysis that positive edge utility (strength) indicates concordant embedding dimensions but high values in dimension 17 for university and low values for vocational education, respectively.

To provide an geographical intuition on which inter-municipality relations were the most important for predicting right-wing populist voting, we show maps of Dutch municipalities with the most positive ( $> 99$ th percentile) and most negative ( $< 1$ st percentile) average edge utilities between them in Fig. 6C. The most positive average edge utilities were between municipalities with larger cities, such as Amsterdam, Rotterdam, and Maastricht, which also had low percentages of right-wing populist votes. The most negative average edge utilities were between rural, smaller municipalities that range from the North-east (e.g., in the province of Drenthe) to the South-west (e.g., in the province of Zeeland). These municipalities tended to have high percentages of right-

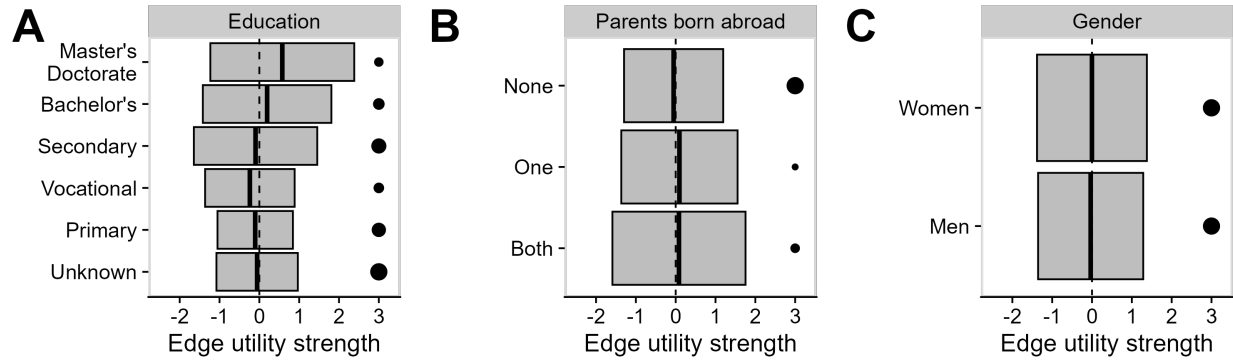


**Figure 5: Edge utility strength for different person-level variables.** Highest achieved education levels (A), the number of parents born outside the Netherlands (B), and gender (C). Bold vertical bars indicate means and boxes span  $\pm 2$  standard deviations from the mean of the edge utility strength distributions. The size of the circles on the right of each box indicate the number of persons in the respective category. The categories are mutually exclusive within each panel but not across panels.

wing populist votes. Thus, relations between persons living in urban as well as remote rural municipalities were the most important for predicting right-wing populist voting.

### Sensitivity Analysis

Both embedding methods that we used rely on random sampling. To see how much our exploratory results depended on the specific embeddings we selected, we repeated the analysis with the DINE-transformed embeddings from the second-best prediction model (see Table A2 for model and embedding hyperparameters and Supplementary Materials for results). The results were overall similar: One transformed embedding dimension was strongly associated with right-wing populist voting (although it was only the third most important predictor after trust in the government and vocational degree). Analyzing edge utility in this dimension revealed similar differences in edge utility between household and classmate relations and no meaningful differences between family relations. Similar to the best model, edge utility strength was on average positive for university and negative for vocational education levels. However, the correlation between edge utility strength and income was higher ( $r = 0.17$ ) than in the best model ( $r = 0.08$ ), suggesting that persons with higher income had more important first-order relations and structural network differences compared to persons with lower income. At the municipality level, correlations between average edge utility strength and municipality statistics were overall lower but similar in rank.

### Discussion

The goal of this study was to create embeddings for an entire population using only network ties reflecting shared social contexts. In the preregistered part of the study, we show that, in line with our expectations, network embeddings predicted a relevant social outcome—right-wing populist voting—above chance level in a representative sample. However, in contrast to what we expected, predictions based on embeddings alone were worse than those based on personality-related and socio-economic covariates, and the embeddings did not improve covariate-based predictions. Nev-

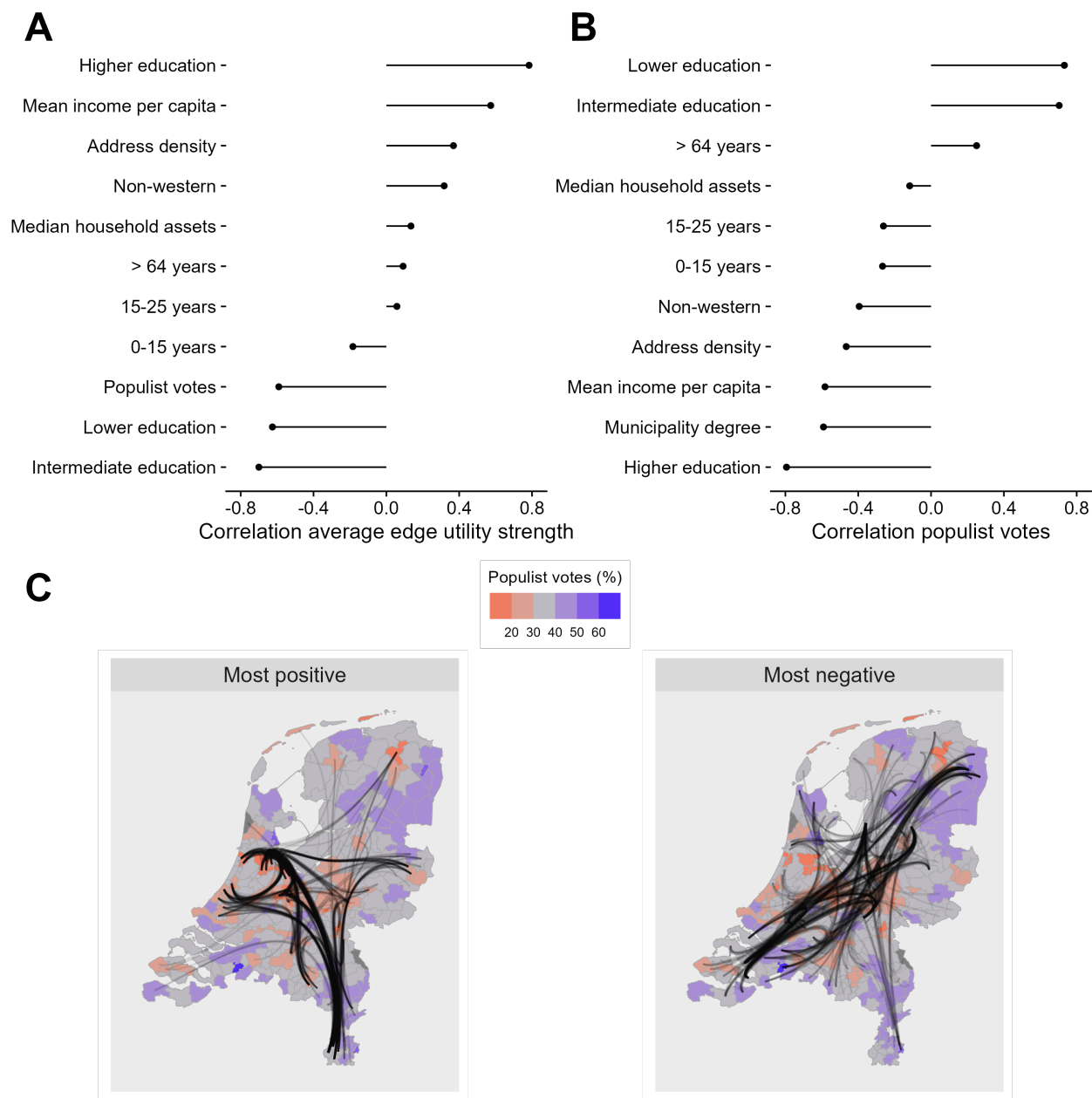


Figure 6: **Average edge utility strength at the municipality level.** Pearson correlations between aggregated municipality statistics and (A) municipality average edge utility strength and (B) right-wing populist votes. C: Maps of the Netherlands and average edge utility connections between Dutch provinces. The right panel shows the most positive connections (top percentile of average edge utility distribution) and the left panel shows the most negative connections (bottom percentile). Color indicates the percentage of votes for a right-wing populist party in each province (gray represents the country-wide average).

ertheless, when looking at a subset of the best-performing embeddings in our exploratory analysis, we found that embeddings slightly improved the prediction performance based on covariates.

In the Supplementary Materials, we also present prediction results for two additional outcomes: general voting behavior and trust in the government. They show similar performance patterns, indicating that the predictive ability of network embeddings generalizes to voting beyond right-wing populist parties and political attitudes related to populist voting [36, 37, 38]. For general voting, the increase in prediction performance from combining embeddings and covariates was slightly larger compared to right-wing populist voting when looking at the best subset of embeddings.

This result shows that our population-scale embeddings encoded information related to right-wing populist voting, but that this information largely overlapped with information contained in established covariates of the outcome (see also [39]). Our exploratory analysis gives insight into which covariates overlapped with our embeddings: We found that one embedding dimension was particularly important for predicting right-wing populist voting, after transforming embedding dimensions using the DINE framework [34]. This “populist” embedding dimension suggests that DINE successfully disentangled the embedding dimensions and that the transformed embeddings are interpretable in the context of a relevant social outcome.

Mapping the “populist” embedding dimension to the population network revealed that institutional household, university, and vocational school relations were more important for predicting right-wing populist voting than others. While connected persons had concordant embedding dimensions with each other, their values in the “populist” dimension differed between these relations. That is, the “populist” dimension captured a similarity in local network structure that was predictive of right-wing populist voting. Moreover, it captured differences in local network structure between persons with a university degree and persons with a vocational degree. Again, while these persons had concordant embedding dimensions with their neighbors, they had different values in the “populist” dimension, indicating that this difference in network structure predicted right-wing populist voting.

Our relation-level results allow for the alternative interpretation that, for university relations, persons were concordant in the “populist” but discordant in the other embedding dimensions. We argue that this interpretation is plausible under special circumstances (e.g., students commuting to a university in a different city) but implausible for the majority of university relations. The same applies to vocational relations, where persons could have been discordant in the “populist” but concordant in the other embedding dimensions. At the person-level, persons with university education could have been discordant while persons with vocational education could have been concordant with their neighbors in embedding dimensions except for the “populist” dimension. However, this would suggest that higher-educated persons were more likely to be isolated in the network while vocational-educated persons were more closely embedded but isolated with respect to voting behavior. We argue that both conditions might hold for a small part of the population but not for the majority (see also [20]). We found support for our interpretation at the municipality level, showing that municipality education levels and percentage of right-wing populist votes were correlated with the “populist” embedding dimension, given that municipality residents had concordant embedding dimensions to their network neighbors.

These results suggests that the association between the “populist” embedding dimension and right-wing populist voting was driven by differences in local network structure related to education. This explains why there was a strong information overlap between embeddings and covariates,

especially, because education levels were among the most important covariates for predicting right-wing populist voting.

The differences in local network structure in education can be explained by homophily, the tendency of persons with similar characteristics to form a tie in a social network [40, 41]. For example, the children of parents with a university degree will be more likely to also obtain a university degree. The results are also consistent with socioeconomic segregation, which previous studies have found in the Dutch population network for education, income, ethnicity, and migration background [17, 42]. However, our study shows that these structural differences also predicted a relevant social outcome, namely, right-wing populist voting.

Our results align with a previous study suggesting that persons with higher socio-economic status are more closely embedded in the Dutch population network and have better access to new social opportunities during their adult life compared to those with lower socio-economic status [20] (and hence a different local network structure). Similar results have been shown for the Danish and Swedish population networks [18, 19].

While demonstrating the usefulness and interpretability of population-scale network embeddings, our study comes with several limitations. The most important limitation stems from the construction of the population network. The network layers differ qualitatively in the probability of resulting in actual interactions between persons. For example, living in the same household is more likely to result in frequent interaction than living in the same neighborhood. Regarding voting behavior and related contagious social outcomes, different layers contain predictive information due to homophily, contagion, and shared environments [43]. By treating the layers equally when creating the embeddings, we likely overshadowed contagion with homophily and shared environment effects, leading to a high information overlap between embeddings and individual characteristics.

Another shortcoming is that registry-based population networks in their current state miss important shared social contexts, such as voluntary associations (e.g., religious groups), that have high probabilities of resulting in frequent interaction [41]. Thus, future studies could explore linking registry networks with other network data sources, for example, donated social media data or representative surveys, and explore their added predictive value [44].

We also faced the problem that not all participants in the LISS panel could be linked to the registry data, for example, because they opted out of the linkage. While this could potentially affect the generalizability of our prediction performance results [44], we did not observe substantial differences in right-wing populist voting before and after the linkage (17.8% vs. 17.9%). However, in the LISS panel data, fewer people indicated that they voted for a right-wing populist party compared to official voting results at the national level (31.1% votes for right-wing populist parties).

We intended the embeddings to be generic individual representations, and including as many ties and information as possible might be beneficial for predicting other social outcomes. We see the embeddings used in this study as a starting point and encourage future studies to test more outcome-specific embeddings, more complex embedding methods (e.g., graph neural networks [45]), or layer-specific embeddings (e.g., layered random walks [46]). Alternatively, future embeddings could be created from a subset of contexts (e.g., only close family relations in the family layer) or shared contexts defined by different rules. While we did not find differences in the predictive performance of embeddings created for years 2020 to 2022, we think it is worthwhile to explore changes in network structure through embeddings over a longer period, extending findings from the Danish population network [18].

We also want to highlight that network embeddings can pave the way to study causal mechanisms at the population scale. They can be used similarly to propensity scores when estimating treatment or contagion effects to account for unobserved confounders but without the need to specify a generative model for the confounding mechanism [47, 48].

Before concluding this article, we want to emphasize that the predictive models in this study were designed as proof-of-concept to show how much predictive information population network embeddings contain compared to other variables and to identify the most important embedding dimensions. They are not intended for deployment, for example, to predict voting outcomes in future elections in the Netherlands. Given that elections can be influenced by political history (e.g., passing certain laws) and external events (e.g., wars) that are not necessarily reflected in the data we used for prediction, we do not know the extent to which our models generalize beyond the election used for training and evaluation.

This study demonstrated that population-scale network embeddings were useful in two complementary ways: They predicted relevant social outcomes, such as right-wing populist voting behavior, although only to a limited extent. We were also able to make them interpretable, revealing embedding dimensions and differences in local network structure that were predictive of social outcomes. Analyzing these differences provided insights into relations between social outcomes and social structure, such as structural differences in education that were associated with right-wing populist voting.

## Methods

We preregistered the methodology and analysis plan of the first part of the study on the Open Science Framework (<https://osf.io/td68b/>). The repository also contains aggregated data that were approved for publication by Statistics Netherlands (see also our Ethics statement). We report deviations from the preregistration in the Supplementary Materials using a template by [49] and assess their impact on the test severity and inference quality of our preregistered analysis [50]. A more detailed explanation of datasets and variables with identifiers can also be found in the Supplementary Materials.

### Data

#### Registry Data

We created node embeddings based on the Dutch population network available through Statistics Netherlands. The nodes in the network represent persons registered in the Netherlands. We used ties from all five available network layers that reflect shared social contexts between persons: A neighbors layer that links individuals to the persons living at the geographically 10 closest addresses (not considering height differences or institutional households with more than 10 members) as well as persons living at one of 20 addresses within 200 meters (the latter are randomly sampled when more than 20 households exist within 200 meters and include institutional households). A colleagues layer connecting a person to the 100 geographically closest persons working for the same employer. A family layer connecting persons with their nuclear (parents and children) and extended family (grandparents, cousins, nephews, nieces, aunts, and uncles). A household layer connecting all persons living in the same household. And a classmates layer which connects persons enrolled in the same institution, institution location, institution type, or educational program (e.g., primary school, university), and study year. Details on the network creation from

registry data, basic network statistics, and data access are described in [17]. While the neighbors and colleagues layers are not necessarily symmetric, we treated them as such by adding reverse connections for each directed connection and filtering for unique connections. We collapsed the five layers into a single undirected, unweighted network (also referred to as *network aggregation* [46]). We justify creating an unweighted network by the low number of persons that are connected in more than one layer (see [20] for layer overlap in the 2018 population network). We created collapsed networks for the years 2020, 2021, and 2022 to allow for comparisons across years.

Besides the network, we used several person-level variables that are available in the registry: Basic demographic variables were age (years since birth year), gender (male, female), and number of parents born outside of the Netherlands (none, one, or both). Socio-economic variables were  $\log(1 + x)$ -transformed purchasing power (i.e., average of income of current and previous year standardized according to prices of current year), change in purchasing power from previous to current year, gross income percentile, and highest achieved educational degree based on aggregation level two of the *Standaard Onderwijsindeling 2021* by Statistics Netherlands (primary, vocational, secondary, Bachelor's or equivalent, Master's or doctorate; see <https://www.cbs.nl/nl-nl/onze-diensten/methoden/classificaties/onderwijs-en-beroepen/standaard-onderwijsindeling--soi--/standaard-onderwijsindeling-2021>).

## Survey Data

In addition to the registry data, we make use of data from the LISS panel (Longitudinal Internet studies for the Social Sciences; [32]; accessed on 17 September 2024), which is administered and managed by the non-profit research institute Centerdata (Tilburg University, Netherlands). The LISS panel is a representative sample of Dutch individuals who participate in monthly internet surveys. The panel is based on a true probability sample of households drawn from the population register by Statistics Netherlands. Self-registration is not possible, and households that would otherwise be unable to participate are provided with a computer and internet connection.

We used data from two modules of the LISS Core Study wave 16 collected between 2023 and 2024. From the Personality module [51], we used the variables happiness, trait mood, state mood, life satisfaction, interpersonal trust, extraversion, emotional stability (i.e., inverse of neuroticism), openness, conscientiousness, agreeableness, self-esteem, interpersonal closeness, social desirability, and optimism.

We created three outcome variables from the Personality and Values module [52]: The first two were trust in the government (“Can you indicate, on a scale from 0 to 10, how much confidence you personally have in each of the following institutions?” with the item “The Dutch government”) and general voting behavior (“For which party did you vote in the parliamentary elections of 22 November 2023?”). Panel participants could choose from a list of 17 national parties, and we added additional categories for missing answers and non-voters. From this variable, we constructed the third outcome “voted for right-wing populist party” by categorizing answers according to (non-) right-wing populist parties, missing, not eligible, or not voted. We used the Populist 3.0 [53] to categorize parties as (non-) right-wing populist. Because version 3.0 of the populist was published in 2022, we classified parties that were not considered in the Populist as non-populist. Since the only left-wing political party classified as populist is the Socialist Party, and it is considered a “borderline populist” party, we decided to exclude it and focus only on right-wing populist parties (i.e., PVV, BBB, Ja21, FvD). For conciseness, we focus on the outcome right-wing populist voting

in the main text and report results on the other two outcomes in the Supplementary Material and refer to them in the discussion.

We used linkage keys provided by Statistics Netherlands to link the panel variables with the registry networks and person-level variables. Some panel participants opted out of the linkage or could not be linked for unknown reasons (13.9%), resulting in a linked panel sample size of 6063 participants. For descriptive statistics of the linked panel and person-level registry variables, see Table A3 and A4. Correlations between variables are provided in the Supplementary Materials.

We removed 136 participants who were not eligible for voting (2.24%; 2.25% before data linkage).

## Network Embeddings

### Embedding Generation

For the undirected, unweighted population network  $\mathcal{G}(\mathcal{V}, \mathcal{E})$ , we created an embedding matrix  $\mathbf{X} \in \mathbb{R}^{D \times |\mathcal{V}|}$  with  $D$  dimensions using two different methods: First, we trained Skip-gram models [54] that predict node pairs in random walk node sequences generated from the network. This method is known as DeepWalk [55]. We trained DeepWalk models on 10 and 100 random walks of length 5, 10, and 20 starting at each node in the network using a context window size of 2, 5, and 8, and embedding dimension 32, 64, and 128. We trained models with 10 walks per node for 20 epochs, and models with 100 walks per node for 2 epochs. We used an initial learning rate of 0.025, a minimum learning rate of 0.0001, and a negative sampling ratio of 5 with an exponent of 0.75. Second, we trained LINE (large-scale information network embedding; [56]) models that predict whether a pair of nodes is a positive sample (they have a connection in the network) or a negative sample (the nodes are randomly sampled). Our LINE models contain embeddings that encode first- and second-order node relationships. First-order embeddings encode local neighborhoods, whereas second-order embeddings capture structural similarity (i.e., nodes with a similar position in their local neighborhood have similar embeddings). We concatenate the two embedding vectors with 8, 16, 24 dimensions, respectively. We used a learning rate of 0.025 and trained for 5 epochs. The negative sampling ratio was 5 with an exponent of 0.75 and the batch size was 100,000 edges.

### Decoupling Embedding Dimensions to Improve Interpretability

We further transformed the embeddings using the DINE framework [34] to obtain orthogonal, sparse, and more interpretable embedding dimensions. In particular, we employed a one-layer autoencoder to learn interpretable node embeddings. For the input embedding matrix  $\mathbf{X}$ , the hidden representation is computed as  $\mathbf{H} = \text{sigmoid}(\mathbf{W}^{(0)}\mathbf{X} + \mathbf{b}^{(0)})$  and the autoencoder reconstructs the input as  $\tilde{\mathbf{X}} = \mathbf{W}^{(1)}\mathbf{H} + \mathbf{b}^{(1)}$ . The hidden layer matrix  $\mathbf{H} \in \mathbb{R}^{D \times |\mathcal{V}|}$  contains the transformed embeddings that we aim to learn. While the original embeddings have range  $(-\infty, \infty)$ , the transformed embeddings have range  $[0, 1]$ .

We trained the autoencoder using the loss function:

$$\mathcal{L} = \text{MSE}(\mathbf{X}, \tilde{\mathbf{X}}) + \mathcal{L}_{orth} + \mathcal{L}_{size}, \quad (1)$$

where  $\mathbf{X}$  and  $\tilde{\mathbf{X}}$  are the original and predicted embedding matrices, respectively.

For each dimension  $d = 1, 2, \dots, D$ , we define edge utility mask matrix  $\mathbf{M}_d \in \mathbb{R}^{|\mathcal{V}| \times |\mathcal{V}|}$  such that for any edge  $(u, v) \in \mathcal{E}$ ,  $\mathbf{M}_d(u, v) = \frac{1}{D} \mathbf{H}(d, u) \cdot \mathbf{H}(d, v)$ . We also define the partition matrix  $\mathbf{P} \in \mathbb{R}^{D \times |\mathcal{V}|}$  with elements  $\mathbf{P}(d, v) = \sum_u \mathbf{M}_d(u, v)$ . The *orthogonality loss*,  $\mathcal{L}_{orth}$ , is designed to



minimize the overlap of encoded structural information in different dimensions and is computed as follows:

$$\mathcal{L}_{orth} = \text{MSE} \left( \frac{\mathbf{P}\mathbf{P}^T}{\|\mathbf{P}\mathbf{P}^T\|_F}, \frac{\mathbf{I}_D}{\|\mathbf{I}_D\|_F} \right), \quad (2)$$

where  $\mathbf{I}_D$  is the identity matrix, and  $\|\cdot\|_F$  is the Frobenius norm.

The *size loss* is introduced to prevent degenerate solutions that might arise from using only the orthogonality loss. For example, without this constraint, the model might assign all important edges to just one embedding dimension, making the others meaningless. To address this, we define a size variable for each dimension  $d$  as  $s_d = \sum_{u,v} \mathbf{M}_d(u, v)$ . This represents the total importance (or summed weight) of all edges in the edge utility mask for dimension  $d$ . To encourage a balanced use of all dimensions, we maximize the entropy of the size variables  $s_d$ :

$$\mathcal{L}_{size} = \log |D| + \sum_d \frac{s_d}{\sum_q s_q} \log \frac{s_d}{\sum_q s_q}, \quad (3)$$

We added a small amount of noise to the input embedding matrix using isotropic Gaussian noise with  $\sigma = 0.2$ . This nudges the auto-encoder to denoise embeddings during the transformation and also augments the training data set since the noise is not constant across epochs. We trained the auto-encoder with a learning rate of 0.1 and a batch size of 10,000 for 50 epochs.

In total, we aimed for 3 (walk length)  $\times$  2 (number of walks)  $\times$  3 (window size)  $\times$  3 (embedding dimension)  $\times$  3 (network year) = 162 DeepWalk representations from which 11 could not be created due to computational issue (6.79%; training DeepWalk embeddings with 128 dimensions, 100 walks per node, and window size 8 exceeded our computational capacities in some cases). Together with 3 (embedding dimension)  $\times$  3 (network year) = 9 LINE representations, this led to 162 - 11 + 9 = 160 different embedding configurations.

### Prediction Performance

We trained models to predict the outcome right-wing populist voting in the LISS panel sample using three feature sets. The first only contained the node embeddings of the LISS participants. The second feature set contained only individual covariates (see section Data), and the third feature set contained both embeddings and covariates.

For prediction, we used three different algorithms: Logistic regression with L2 regularization, k-nearest neighbor classification, and XGBoost classification. In total, we trained 2 (transformed yes/no)  $\times$  3 (embedding feature sets)  $\times$  160 (embeddings)  $\times$  3 (prediction algorithm) = 2880 predictive models for right-wing populist voting.

For logistic regression and k-nearest neighbor classification, missing continuous predictor values were imputed using the median. For all algorithms, missing categorical predictor values were added as a separate category.

We assessed the performance of the predictive models using nested stratified cross-validation (CV) with 5 inner and 5 outer folds. As the performance metric, we used the macro area under the curve (AUC) score for right-wing populist voting (unweighted average of AUC scores for each outcome class). We computed outcome class probabilities using one-vs-rest classification. We optimized hyperparameters of the predictive models using the average score in the inner CV loop using the Optuna framework [57] with 100 iterations. The hyperparameter ranges are specified in Table A5.

To compare the performance of different predictive models, we estimated a Bayesian regression model to predict their outer CV loop macro AUC scores:

$$\text{score} \sim \text{algorithm} \times \text{feature\_set} + \text{transformed} + \text{year} + \text{walk\_length} \times \text{num\_walks} \\ + \text{window\_size} + \text{embedding\_dim}.$$

Because AUC scores fall between 0 and 1, we used a generalized linear regression model with a beta family and logit link function. The nuisance parameter  $\phi$  of the beta distribution was estimated as  $\phi \sim \text{algorithm} \times \text{feature\_set}$  to allow for different variances in AUC scores between prediction algorithms and feature sets. Missing scores were estimated as additional parameters by the regression model. All independent variables were categorical. We used  $N(0, 2.5)$  as weakly informative prior distributions for the regression coefficients and  $\text{Exp}(1)$  on the parameters for estimating  $\phi$ . For non-applicable predictor combinations, we restricted regression coefficients to zero (e.g., only prediction models with embeddings in their feature set had embedding hyperparameter values). We assessed the posterior predictive distribution of the regression model and concluded that the predicted scores aligned sufficiently with the observed CV scores (see Supplementary Materials).

### Exploratory Analysis

To investigate which connectivity patterns in the network are relevant for predicting our outcome variables, we used a modified version of the workflow described in [34]: First, we retrained the prediction model with DINE-transformed embeddings and the best average prediction score for populist voting in the outer CV loop on the entire LISS panel data using only one stratified CV loop to optimize the hyperparameters as we did with previous models. Then, we calculated SHAP [58, 59] feature importance scores for this model to assess how much each predictor contributed to the model predictions. We calculated SHAP values for each class and restricted the analysis to the scores for the populist class. From the predictors for each outcome, we selected the DINE-transformed embedding dimension with the highest mean absolute SHAP values for the subsequent analyses.

We calculated edge utility scores for the selected dimension and all edges in the network [34]. The edge utility  $\mu_d(u, v)$  quantifies the marginal contribution of dimension  $d$  to the similarity between the embeddings of the source and target node in the edge  $(u, v)$  (see also Fig. 1C):

$$\mu_d(u, v) = \Delta_D(u, v) - \Delta_{D \setminus \{d\}}(u, v), \quad (4)$$

where  $\Delta_D(u, v)$  is the average embedding score of the edge, the (unnormalized) similarity between nodes  $u$  and  $v$ :

$$\Delta_D(u, v) = \frac{1}{D} \mathbf{H}(u) \cdot \mathbf{H}(v), \quad (5)$$

and  $\Delta_{D \setminus \{d\}}(u, v)$  the similarity between nodes  $u$  and  $v$  excluding the dimension  $d$ .

Edge utility is positive (negative) when the similarity in dimension  $d$  is above (below) the average similarity over all dimensions. Thus, edge utility is positive when either (a) all dimensions are concordant but  $d$  has a higher value than the other dimensions or (b) dimension  $d$  is concordant but the other dimensions are discordant. In contrast, edge utility is negative when either (a) all dimensions are concordant but  $d$  has a lower value than the other dimensions or (b) dimension  $d$  is discordant but the other dimensions are concordant.

We interpret edge utility as a measure of how important edges are for predicting right-wing populist voting, given that it is highly associated with the selected embedding dimension.

We aggregate edge utility at the person-level by defining edge utility strength as the sum of first-order edge utilities in dimension  $d$ :

$$S_d(u) = \sum_v \mu_d(u, v). \quad (6)$$

Values different from zero indicate that a person has first-order relations that are important for predicting right-wing populist voting. We interpret edge utility strength as an indicator of differences in network structure that are predictive of right-wing populist voting.

Lastly, we aggregated edge utility at the municipality level (in total 342 municipalities) by averaging over edges that have source and target nodes in the same or a different municipality:

$$\gamma_d(m, n) = \frac{1}{|\mathcal{E}'|} \sum \mu_d(u_m, v_n), \quad (7)$$

where  $\mathcal{E}'$  is the subset of edges that connect persons from municipalities  $m$  and  $n$ . We then calculated the average edge utility strength for each municipality:

$$Q_d(m) = \sum_n \gamma_d(m, n). \quad (8)$$

We correlated municipality-level average edge utility strength with aggregated municipality statistics: Mean income per capita, median household assets, address density, population share in three age groups (0-15, 14-25, > 64 years), population share of highest achieved educational degree (lower, intermediate, higher), and population share with a non-western migration background. Additionally, we obtained the percentage of votes for populist parties in each municipality in the Netherlands for the parliamentary election on November 22nd, 2023.

**Supplementary Materials** Supplementary Materials are available at <https://github.com/odissei-explainable-network/netaudit>.

**Acknowledgements** We would like to thank ODISSEI (the Open Data Infrastructure for Social Sciences and Economic Innovations) for making administrative registry data more accessible. ODISSEI also provided data access for this project (grant number 184.035.014). The LISS panel data were collected by the non-profit research institute Centerdata (Tilburg University, the Netherlands). Funding for the panel's ongoing operations comes from the Domain Plan SSH and ODISSEI since 2019. The initial set-up of the LISS panel in 2007 was funded through the MESS project by the Netherlands Organization for Scientific Research (NWO). Javier Garcia-Bernardo acknowledges support from NWO (grant number VI.Veni.231S.148).

## Funding

Funding was provided by ODISSEI through a microdata access grant awarded to MK (grant number 184.035.014) and by the Netherlands Organization for Scientific Research (NWO) to JGB (grant number VI.Veni.231S.148).

## Competing Interests

The authors have no competing interests to declare.

## Ethics Statement

Ethics approval was obtained from the Human Research Ethics Committee at Delft University of Technology on June 9th 2024 (application number 4403). All analyses on raw registry data were conducted in the secure remote access environment by Statistics Netherlands (project number 9780). In this environment, all personal data is pseudonomized. All results presented in this study were checked by Statistics Netherlands for risks of personal information disclosure and approved for publication (for details on privacy, see <https://www.cbs.nl/nl-nl/over-ons/dit-zijn-wij/onze-organisatie/privacy>). To prevent disclosure of personal information, only aggregated, fully anonymized results are presented in this study.

## Consent for Publication

Not applicable.

## Data Availability

The raw datasets used in this study are not openly available. The Dutch population network and registry data can be accessed through Statistics Netherlands under certain conditions (for details, see <https://www.cbs.nl/nl-nl/onze-diensten/maatwerk-en-microdata/microdata-zelf-onderzoek-doen>). The LISS Panel data can be accessed through the LISS Archive (see <https://www.lissdata.nl/how-it-works-archive>). The embeddings that were created as part of this study are archived in the Data Storage Facility from Statistics Netherlands and ODISSEI. They can also be accessed through Statistics Netherlands with consent from the authors. The metadata for the embeddings can be found here:

- DeepWalk embeddings: <https://doi.org/10.34894/VRNLKJ>
- DeepWalk embeddings DINE transformed: <https://doi.org/10.34894/DRRGIV>
- LINE embeddings: <https://doi.org/10.34894/RVVTRB>
- LINE embeddings DINE transformed: <https://doi.org/10.34894/9JLZ4E>

Aggregated data that has been checked for risks of personal information disclosure and approved by Statistics Netherlands is available at <https://github.com/odissei-explainable-network/netaudit>.

Municipality statistics are openly available via CBS Open Data StatLine ([https://opendata.cbs.nl/statline/portal.html?\\_la=nl&\\_catalog=CBS&tableId=85039NED&\\_theme=246](https://opendata.cbs.nl/statline/portal.html?_la=nl&_catalog=CBS&tableId=85039NED&_theme=246)). Municipality-aggregated voting data are openly available via the Overheid.nl website (<https://data.overheid.nl/dataset/verkiezingsuitslag-tweede-kamer-2023>).

## Materials Availability

Not applicable.

## Code Availability

Code is available at <https://github.com/odissei-explainable-network/netaudit>.

## Author Contributions

ML, JGB, and MK conceptualized the study. MK acquired funding and supervised the project together with JGB. ML, SD, and FH wrote the software necessary for executing the study. ML conducted the data analysis. ML, JGB, FH, and MK wrote the manuscript which was reviewed and approved by all authors.

## References

- [1] Höcük, S., Kumar, P., Mulder, J. & Prüfer, P. Economies of scope in the aggregation of health-related data. *JRC Digital Economy Working Paper* (2021). URL <https://hdl.handle.net/10419/266521>.
- [2] Kunaschk, M. Enriching administrative data using survey data and machine learning techniques. *Economics Letters* **243**, 111924 (2024). URL <https://www.sciencedirect.com/science/article/pii/S0165176524004087>.
- [3] Narayanan, A., Stewart, T., Duncan, S. & Pacheco, G. Using machine learning to explore the efficacy of administrative variables in prediction of subjective-wellbeing outcomes in New Zealand. *Scientific Reports* **15** (2025). URL <https://doi.org/10.1038/s41598-025-90852-0>.
- [4] Kuikka, S. The (un)predictability of early (un)employment: A machine learning approach. *Socius* **10**, 23780231241286655 (2024). URL <https://doi.org/10.1177/23780231241286655>.
- [5] Hansen, A. V., Mortensen, L. H., Ekstrøm, C. T., Trompet, S. & Westendorp, R. Predicting mortality and visualizing health care spending by predicted mortality in Danes over age 65. *Scientific Reports* **13**, 1203 (2023). URL <https://doi.org/10.1038/s41598-023-28102-4>.
- [6] Burger, J., Boonstra, H. J. & van den Brakel, J. Effect of spatial scale, color infrared and sample size on learning poverty from aerial images. *Remote Sensing Applications: Society and Environment* **36**, 101304 (2024). URL <https://www.sciencedirect.com/science/article/pii/S235293852400168X>.
- [7] Echevin, D., Fotso, G., Bouroubi, Y., Coulombe, H. & Li, Q. Combining survey and census data for improved poverty prediction using semi-supervised deep learning. *Journal of Development Economics* **172**, 103385 (2025). URL <https://www.sciencedirect.com/science/article/pii/S0304387824001342>.
- [8] Savcicens, G. *et al.* Using sequences of life-events to predict human lives. *Nature Computational Science* **4**, 43–56 (2023). URL <https://doi.org/10.1038/s43588-023-00573-5>.

- [9] Sivak, E. *et al.* Combining the strengths of Dutch survey and register data in a data challenge to predict fertility (PreFer). *Journal of Computational Social Science* **7**, 1403–1431 (2024). URL <https://doi.org/10.1007/s42001-024-00275-6>.
- [10] Ericsson, L., Gouk, H., Loy, C. C. & Hospedales, T. M. Self-supervised representation learning: Introduction, advances, and challenges. *IEEE Signal Processing Magazine* **39**, 42–62 (2022). URL <https://ieeexplore.ieee.org/document/9770283/>.
- [11] Bengio, Y., Courville, A. & Vincent, P. Representation learning: A review and new perspectives. *IEEE Transactions on Pattern Analysis and Machine Intelligence* **35**, 1798–1828 (2013). URL <https://ieeexplore.ieee.org/document/6472238/>.
- [12] Zhang, D., Yin, J., Zhu, X. & Zhang, C. Network representation learning: A survey. *IEEE Transactions on Big Data* **6**, 3–28 (2020). URL <https://ieeexplore.ieee.org/document/8395024/>.
- [13] Granovetter, M. The impact of social structure on economic outcomes. *Journal of Economic Perspectives* **19**, 33–50 (2005). URL <https://pubs.aeaweb.org/doi/10.1257/0895330053147958>.
- [14] Smith, K. P. & Christakis, N. A. Social networks and health. *Annual Review of Sociology* **34**, 405–429 (2008). URL <https://www.annualreviews.org/doi/10.1146/annurev.soc.34.040507.134601>.
- [15] Lazer, D. Networks in political science: Back to the future. *PS: Political Science & Politics* **44**, 61–68 (2011). URL [https://www.cambridge.org/core/product/identifier/S1049096510001873/type/journal\\_article](https://www.cambridge.org/core/product/identifier/S1049096510001873/type/journal_article).
- [16] Stulp, G., Top, L., Xu, X. & Sivak, E. A data-driven approach shows that individuals’ characteristics are more important than their networks in predicting fertility preferences. *Royal Society Open Science* **10**, 230988 (2023). URL <https://royalsocietypublishing.org/doi/10.1098/rsos.230988>.
- [17] van der Laan, J., de Jonge, E., Das, M., Te Riele, S. & Emery, T. A whole population network and its application for the social sciences. *European Sociological Review* **39**, 145–160 (2023). URL <https://doi.org/10.1093/esr/jcac026>.
- [18] Cremers, J. *et al.* Unveiling the social fabric: A temporal, nation-scale social network and its characteristics (2024). Preprint at <http://arxiv.org/abs/2409.11099>.
- [19] Panayiotou, G. *et al.* Anatomy of a Swedish population-scale network (2025). Preprint at [https://osf.io/qsr24\\_v1](https://osf.io/qsr24_v1).
- [20] Bokányi, E., Heemskerk, E. M. & Takes, F. W. The anatomy of a population-scale social network. *Scientific Reports* **13**, 9209 (2023). URL <https://www.nature.com/articles/s41598-023-36324-9>.

- [21] Van Holsteyn, J. J. M. & Irwin, G. A. The Dutch parliamentary elections of November 2023. *West European Politics* **48**, 464–477 (2025). URL <https://www.tandfonline.com/doi/full/10.1080/01402382.2024.2397629>.
- [22] Lazarsfeld, P. F., Berelson, B. & Gaudet, H. *The people's choice: How the voter makes up his mind in a presidential campaign* (Columbia University Press, New York, 2019).
- [23] Sinclair, B. *The social citizen: Peer networks and political behavior*. Chicago studies in American politics (University of Chicago Press, Chicago, 2012).
- [24] Arias, E., Balán, P., Larreguy, H., Marshall, J. & Querubín, P. Information provision, voter coordination, and electoral accountability: Evidence from mexican social networks. *American Political Science Review* **113**, 475–498 (2019). URL [https://www.cambridge.org/core/product/identifier/S0003055419000091/type/journal\\_article](https://www.cambridge.org/core/product/identifier/S0003055419000091/type/journal_article).
- [25] Alt, J. E., Jensen, A., Larreguy, H., Lassen, D. D. & Marshall, J. Diffusing political concerns: How unemployment information passed between social ties influences Danish voters. *The Journal of Politics* **84**, 383–404 (2022). URL <https://www.journals.uchicago.edu/doi/10.1086/714925>.
- [26] Berelson, B. *Voting: A study of opinion formation in a presidential campaign* (University of Chicago Press, Chicago, 1954).
- [27] Huckfeldt, R. R. & Sprague, J. *Citizens, politics and social communication: Information and influence in an election campaign* (Cambridge University Press, Cambridge, 1995).
- [28] Knoke, D. Networks of political action: Toward theory construction. *Social Forces* **68**, 1041–1063 (1990). URL <https://www.jstor.org/stable/2579133>.
- [29] Burstein, P. Social networks and voting: Some Israeli data. *Social Forces* **54**, 833–847 (1976). URL <https://www.jstor.org/stable/2576178>.
- [30] Bond, R. M. *et al.* A 61-million-person experiment in social influence and political mobilization. *Nature* **489**, 295–298 (2012). URL <https://www.nature.com/articles/nature11421>.
- [31] Nickerson, D. W. Is voting contagious? Evidence from two field experiments. *American Political Science Review* **102**, 49–57 (2008). URL [https://www.cambridge.org/core/product/identifier/S0003055408080039/type/journal\\_article](https://www.cambridge.org/core/product/identifier/S0003055408080039/type/journal_article).
- [32] Scherpenzeel, A. C. & Das, M. “True” longitudinal and probability-based internet panels: Evidence from the Netherlands. In Das, M., Ester, P. & Kaczmirek, L. (eds.) *Social and behavioral research and the internet: Advances in applied methods and research strategies*, 77–104 (Taylor & Francis, New York, 2010).
- [33] Locatello, F. *et al.* Challenging common assumptions in the unsupervised learning of disentangled representations. *Proceedings of the 36th International Conference on Machine Learning* 4114–4124 (2019). URL <https://proceedings.mlr.press/v97/locatello19a.html>.

- [34] Piaggese, S., Khosla, M., Panisson, A. & Anand, A. DINE: Dimensional interpretability of node embeddings. *IEEE Transactions on Knowledge and Data Engineering* **36**, 7986–7997 (2024). URL <https://ieeexplore.ieee.org/abstract/document/10591463>.
- [35] Berman, S. The causes of populism in the west. *Annual Review of Political Science* **24**, 71–88 (2021). URL <https://www.annualreviews.org/doi/10.1146/annurev-polisci-041719-102503>.
- [36] Mounk, Y. *The people vs. democracy: Why our freedom is in danger and how to save it* (Harvard University Press, Cambridge, Massachusetts, 2018).
- [37] Ivanov, D. Economic insecurity, institutional trust and populist voting across europe. *Comparative Economic Studies* **65**, 461–482 (2023). URL <https://link.springer.com/10.1057/s41294-023-00212-y>.
- [38] Colloca, P., Roccato, M. & Russo, S. Rally ‘round the flag effects are not for all: Trajectories of institutional trust among populist and non-populist voters. *Social Science Research* **119**, 102986 (2024). URL <https://www.sciencedirect.com/science/article/pii/S0049089X24000085>.
- [39] Bakker, B. N., Rooduijn, M. & Schumacher, G. The psychological roots of populist voting: Evidence from the United States, the Netherlands and Germany. *European Journal of Political Research* **55**, 302–320 (2016). URL <https://onlinelibrary.wiley.com/doi/abs/10.1111/1475-6765.12121>.
- [40] McPherson, M., Smith-Lovin, L. & Cook, J. M. Birds of a feather: Homophily in social networks. *Annual Review of Sociology* **27**, 415–444 (2001). URL <https://www.jstor.org/stable/2678628>.
- [41] McPherson, J. M. & Smith-Lovin, L. Homophily in voluntary organizations: Status distance and the composition of face-to-face groups. *American Sociological Review* **52**, 370–379 (1987). URL <https://www.jstor.org/stable/2095356>.
- [42] Kazmina, Y., Heemskerk, E. M., Bokányi, E. & Takes, F. W. Socio-economic segregation in a population-scale social network. *Social Networks* **78**, 279–291 (2024). URL <https://www.sciencedirect.com/science/article/pii/S0378873324000157>.
- [43] Shalizi, C. R. & Thomas, A. C. Homophily and contagion are generically confounded in observational social network studies. *Sociological Methods & Research* **40**, 211–239 (2011). URL <https://doi.org/10.1177/0049124111404820>.
- [44] Sakshaug, J. W. & Struminskaya, B. Augmenting surveys with paradata, administrative data, and contextual data. *Public Opinion Quarterly* **87**, 475–479 (2023). URL <https://doi.org/10.1093/poq/nfad026>.
- [45] Corso, G., Stark, H., Jegelka, S., Jaakkola, T. & Barzilay, R. Graph neural networks. *Nature Reviews Methods Primers* **4**, 17 (2024). URL <https://www.nature.com/articles/s43586-024-00294-7>.



- [46] Liu, W., Chen, P.-y., Yeung, S., Suzumura, T. & Chen, L. Principled multilayer network embedding. *2017 IEEE International Conference on Data Mining Workshops (ICDMW)* 134–141 (2017). URL <https://ieeexplore.ieee.org/document/8215654/>.
- [47] Veitch, V., Wang, Y. & Blei, D. Using embeddings to correct for unobserved confounding in networks. *Advances in Neural Information Processing Systems* **32** (2019). URL [https://proceedings.neurips.cc/paper\\_files/paper/2019/hash/af1c25e88a9e818f809f6b5d18ca02e2-Abstract.html](https://proceedings.neurips.cc/paper_files/paper/2019/hash/af1c25e88a9e818f809f6b5d18ca02e2-Abstract.html).
- [48] Cristali, I. & Veitch, V. Using embeddings for causal estimation of peer influence in social networks. *Advances in Neural Information Processing Systems* **35** (2022). URL [https://proceedings.neurips.cc/paper\\_files/paper/2022/file/64587794695be22545d91c838243fcf8-Paper-Conference.pdf](https://proceedings.neurips.cc/paper_files/paper/2022/file/64587794695be22545d91c838243fcf8-Paper-Conference.pdf).
- [49] Willroth, E. C. & Atherton, O. E. Best laid plans: A guide to reporting preregistration deviations. *Advances in Methods and Practices in Psychological Science* **7**, 25152459231213802 (2024). URL <https://doi.org/10.1177/25152459231213802>.
- [50] Lakens, D. When and how to deviate from a preregistration. *Collabra: Psychology* **10**, 117094 (2024). URL <https://online.ucpress.edu/collabra/article/10/1/117094/200749/When-and-How-to-Deviate-From-a-Preregistration>.
- [51] Miquelle Marchand. LISS panel- Personality - Wave 16 (2024). URL <https://doi.org/10.57990/c63p-1250>. Publisher: Centerdata.
- [52] Suzan Elshout. LISS panel - Politics and Values - Wave 16 (2024). URL <https://doi.org/10.57990/xhw0-9614>. Publisher: Centerdata.
- [53] Rooduijn, M. *et al.* The PopuList: A database of populist, far-left, and far-right parties using expert-informed qualitative comparative classification (EiQCC). *British Journal of Political Science* **54**, 969–978 (2024). URL <https://doi.org/10.1017/S0007123423000431>.
- [54] Mikolov, T., Sutskever, I., Chen, K., Corrado, G. S. & Dean, J. Distributed representations of words and phrases and their compositionality. *Advances in Neural Information Processing Systems* **26** (2013). URL <https://proceedings.neurips.cc/paper/2013/hash/9aa42b31882ec039965f3c4923ce901b-Abstract.html>.
- [55] Perozzi, B., Al-Rfou, R. & Skiena, S. DeepWalk: Online learning of social representations. *Proceedings of the 20th ACM SIGKDD international conference on Knowledge discovery and data mining* 701–710 (2014). URL <https://dl.acm.org/doi/10.1145/2623330.2623732>.
- [56] Tang, J. *et al.* LINE: Large-scale information network embedding. *Proceedings of the 24th International Conference on World Wide Web* 1067–1077 (2015).
- [57] Akiba, T., Sano, S., Yanase, T., Ohta, T. & Koyama, M. Optuna: A next-generation hyperparameter optimization framework. *Proceedings of the 25th ACM SIGKDD International Conference on Knowledge Discovery and Data Mining* (2019). URL <https://doi.org/10.1145/3292500.3330701>.

- [58] Štrumbelj, E. & Kononenko, I. Explaining prediction models and individual predictions with feature contributions. *Knowledge and Information Systems* **41**, 647–665 (2014). URL <https://doi.org/10.1007/s10115-013-0679-x>.
- [59] Lipovetsky, S. & Conklin, M. Analysis of regression in game theory approach. *Applied Stochastic Models in Business and Industry* **17**, 319–330 (2001). URL <https://onlinelibrary.wiley.com/doi/abs/10.1002/asmb.446>.

## Appendix

Table 1: Simple Contrasts for Prediction Performance Scores

Contrast		Difference	95% CI	
Level 1	Level 2		Lower	Upper
Estimator				
LinReg	KNN	<b>0.047</b>	0.046	0.047
XGB	KNN	<b>0.058</b>	0.058	0.059
XGB	LinReg	<b>0.012</b>	0.011	0.012
Feature set				
Embed	Cov	<b>-0.09</b>	-0.09	-0.089
Embed + Cov	Cov	<b>-0.012</b>	-0.013	-0.012
Embed + Cov	Embed	<b>0.077</b>	0.077	0.078
Year				
2021	2020	0.00014	-0.00069	0.00096
2022	2020	-0.00026	-0.0011	0.00059
2022	2021	-0.0004	-0.0012	0.00043
DINE-transformed				
Yes	No	-0.0005	-0.0012	0.00016
DeepWalk walk length				
20	10	<b>0.0018</b>	0.00089	0.0027
5	10	<b>-0.0091</b>	-0.01	-0.0083
5	20	<b>-0.011</b>	-0.012	-0.01
DeepWalk walks per node				
100	10	<b>0.0073</b>	0.0065	0.008
DeepWalk window size				
5	2	0.00042	-0.00043	0.0013
8	2	-0.00039	-0.0013	0.00046
8	5	-0.00081	-0.0017	0.000054
Method				
DeepWalk	LINE	<b>0.006</b>	0.0045	0.0076
Dimension				
24	16	0.0032	-0.00034	0.0067
8	16	<b>-0.01</b>	-0.014	-0.0068
8	24	<b>-0.014</b>	-0.017	-0.01
32	128	<b>0.0077</b>	0.0067	0.0086
64	128	<b>0.0036</b>	0.0027	0.0045
64	32	<b>-0.004</b>	-0.0048	-0.0032

Differences in macro AUC score. Positive difference values indicate that the marginal predictions for level 1 are higher than those for level 2. Differences for which the 95% quantile credible interval (CI) excludes zero are highlighted in bold. KNN = k-nearest neighbor. LinReg = linear regression. XGB = XGBoost. Embed = embeddings. Cov = covariates.

Table 2: Configurations of Prediction Models Used in Exploratory and Sensitivity Analyses

	Model exploratory analysis	Model sensitivity analysis
Feature set	Embeddings + covariates	Embeddings + covariates
Algorithm	XGBoost	XGBoost
DINE-transformed	Yes	Yes
Network year	2021	2022
Embedding method	DeepWalk	DeepWalk
Walks per node	100	100
Walk length	20	20
Window size	5	2
Dimensions	32	32
Mean test macro AUC	0.743	0.739

Table 3: Summary Statistics for Numeric Variables in Linked Dataset

Variable	Mean	SD	Missing
Satisfaction 1	4.97	1.26	1226
Happiness	7.32	1.41	1330
Agreeableness	6.73	4.5	1250
Purch power (log)	10.47	0.41	187
Social desirability	1.13	1.97	1274
Satisfaction 2	5.12	1.27	1226
Satisfaction 5	4.52	1.62	1226
Mood trait	5.57	1.01	1226
Emotional stability	-0.17	3.28	1250
Change purch. power	259372.52	4262177.66	187
Satisfaction 4	5.25	1.27	1226
Extraversion	1.69	6.79	1250
Age	51.99	18.82	NA
Interpersonal trust	5.91	2.31	1333
Optimism	2.49	3.72	1276
Satisfaction 3	5.36	1.19	1226
Closeness	4.44	1.56	1271
Trust government	4.73	2.28	709
Openness	4.72	3.48	1250
Conscientiousness	6.02	4.91	1250
Mood state	5.41	1.18	1225
Income percentile	54.92	28.1	284
Self esteem	14.14	10.74	1253

Total sample size was 6063. NA = value not published for privacy reasons.

Table 4: Summary Statistics for Categorical Variables in Linked Dataset

Variable	Level	n	Proportion
Parents born abroad	Zero	NA	NA
	Both	816	0.1346
	One	529	0.0873
	Missing	NA	NA
Gender	Female	3254	0.5367
	Male	NA	NA
	Missing	NA	NA
General voting	GL/PvdA	941	0.1552
	PVV	855	0.141
	Missing	826	0.1362
	Vvd	683	0.1127
	NSC	628	0.1036
	Not voted	520	0.0858
	D66	310	0.0511
	CDA	200	0.033
	SP	186	0.0307
	BBB	155	0.0256
	PvdD	152	0.0251
	Not eligible	136	0.0224
	CU	103	0.017
	Volt	87	0.0143
	SGP	78	0.0129
	Other	64	0.0106
	DENK	49	0.0081
	FvD	47	0.0078
	JA21	27	0.0045
	Blank	16	0.0026
Voted	Yes	4685	0.7727
	Missing	722	0.1191
	No	520	0.0858
	Not eligible	136	0.0224
Right-wing populist voting	Non populist	3497	0.5768
	Populist	1084	0.1788
	Missing	826	0.1362
	Not voted	520	0.0858
	Not eligible	136	0.0224
Highest achieved education	Missing	1877	0.3096
	Higher vocational	1564	0.258
	Bachelor	1200	0.1979
	Master/doctorate	762	0.1257
	Vocational	470	0.0775
	Primary	190	0.0313

Total sample size was 6063. NA = value not published for privacy reasons.

Table 5: Prediction Algorithm Hyperparameter Ranges

Algorithm	Hyperparameter	Lower	Upper
Logistic regression	L2 regularization (inverse) <sup>a</sup>	0.001	100
K-nearest neighbors	Number of neighbors	2	100
XGBoost	Learning rate	0	1
	Maximum depth	2	50
	Minimum child weight	1	100
	Subsample rows	0.2	1
	Subsample columns (by tree)	0.2	1
	Subsample columns (by level)	0.2	1
	L2 regularization <sup>a</sup>	0.001	100

<sup>a</sup> Values were sampled on the log scale.